Colloid Polym Sci (2015) 293:1877–1886
DOI 10.1007/s00396-015-3576-x

ORIGINAL CONTRIBUTION

Adsorption characteristics of anionic azo dye onto large α-alumina beads

Tien Duc Pham[1,2] · **Motoyoshi Kobayashi**[2] · **Yasuhisa Adachi**[2]

Received: 11 February 2015 / Revised: 10 March 2015 / Accepted: 17 March 2015 / Published online: 7 April 2015

Abstract Adsorption of anionic azo dye, new coccine (NC), onto large α-alumina beads in aqueous media was systematically investigated as functions of pH and NaCl concentration. Adsorption amounts of NC decrease with increasing pH of solutions due to less positive charges of α-Al_2O_3 surface at high pH. At a fixed pH, the NC adsorption increases with decreasing NaCl concentration, indicating that NC molecules mainly adsorb onto α-Al_2O_3 by electrostatic attraction. Experimental results of NC adsorption isotherms onto α-Al_2O_3 at different pH, and ionic strength can be represented well by two-step adsorption model. The effects of NC on surface charge and surface modification of α-Al_2O_3 at the plateau adsorption are evaluated by streaming potential and Fourier transform infrared spectroscopy with attenuated total reflection technique (FTIR-ATR), respectively. On the basis of adsorption isotherms, surface charge effect, and surface modification, we suggested that the formation of a bridged bidentate complex between aluminum ions of α-Al_2O_3 and two oxygen atoms of a sulfonic group induced the adsorption of NC onto α-Al_2O_3.

Keywords Anionic dye adsorption · α-Alumina · Surface charge effect · FTIR-ATR · Two-step adsorption model

Introduction

The treatment of wastewater is important in environmental engineering. Organic dyes are the pollutants produced from many industrial activities related to paint, textile, pulp and paper, cosmetic, etc. [1]. Many dye wastes are colored and extremely toxic [1, 2]. Various treatment techniques have been used for the dyes' removal from aquatic environment [3, 4] like adsorption [5–8], photocatalytic degradation [9–11], electrochemical oxidation [12, 13], coagulation/flocculation [14], and biological process [15]. Among them, adsorption is one of the most common technologies for treating ionic dyes in solutions. This technique can be applicable for developing countries by using cheap adsorbents or modified solid waste adsorbents [3, 4, 7, 16]. To enhance the removal efficiency of ionic dyes by modification of adsorbent surface, an understanding of adsorption characteristics of organic dye onto charged solid surfaces is needed.

The investigations on the adsorption characterizations of ionic dyes onto solid surfaces are of great importance to predict mechanism of this process. However, the adsorption properties of ionic dyes are rather complicated due to the complex structures of adsorbed layers when dye molecules have a number of charged groups [2]. Adsorption of charged adsorbates is more complex when the surface charges of solid adsorbents such as metal oxides are regulated by concomitant proton adsorption [17–20]. The charge adjustment of metal oxides upon ionic dyes adsorption has not been obtained. But adsorption characteristics of multivalent organic dyes onto charged metal oxides surface are still inadequate. Wang et al. [21] investigated the effect of pH, suspended solid, and salt concentration on the adsorption properties of trianion of new coccine (NC) dye onto sludge particulates thoroughly. Nevertheless, they have not investigated the change in zeta potential upon

---

✉ Tien Duc Pham
tienduchphn@gmail.com

[1] Faculty of Chemistry, Hanoi University of Science, Vietnam National University, Hanoi, 19 Le Thanh Tong, Hoan Kiem, Hanoi 10000, Vietnam

[2] Graduate School of Life and Environmental Sciences, University of Tsukuba, Tennodai 1-1-1, Tsukuba, Ibaraki 305-8572, Japan

the dye adsorption, the surface modification after dye adsorption, and the structure of adsorbed NC [21].

Many studies focused on adsorption of ionic dyes on metal oxides by combining electrokinetic and spectroscopic measurements with modeling [22–24]. While electrokinetic measurements can provide the information about charging behavior of metal oxides in the absence and presence of ionic dyes, spectroscopic methods can show the active groups on the surface of adsorbent after adsorption and evaluate the adsorption amount of dyes. Furthermore, the isotherms fitted by theoretical models are useful to better understand the adsorption mechanism and to explain the interaction between the surface of metal oxides and ionic dyes. As for describing adsorption characteristics of organic dyes, Langmuir and Freundlich isotherm models are often discussed. Nevertheless, Langmuir and Freundlich models cannot be applied for S shape adsorption isotherms, for example, adsorption of cationic dye, methylene blue on silica sand [25]. Fortunately, a two-step adsorption model presented by Zhu et al. [26] could describe these curves. Based on the two-step model, a general adsorption isotherm equation can be derived. This equation was successfully applied to numerous types of surfactant and polymer adsorption isotherms for various systems [26–29]. The multilayer model which was introduced by the Brunauer–Emmett–Teller (BET) [30] was used to describe adsorption isotherms of the ionic dyes [21, 31–33]. However, the complex multilayer adsorption of ionic dyes fitted by the general equation has not been reported.

Alumina was used as a substrate for adsorption of anionic dyes [34–36]. The adsorption of monovalent azo dyes on alumina is controlled by a bidentate complex [22] while the adsorption of cationic dye on alumina and surfactant-modified alumina is mainly promoted by electrostatic interaction and probably by hydrophobic interaction [1]. The adsorption properties of anionic azo dye onto alumina are more complicated when sorbents are large beads with low surface area. While the adsorption of organic ions on negatively charged surface such as glass beads has attracted numerous researches, not so many studies have been conducted on positively charged large beads. Therefore, we focused on large alumina beads with positively charged surface to better understand the adsorption properties. Furthermore, the use of large oxide beads as a model system can be applied to study transport in porous media [37, 38].

The aim of the present work is to investigate the adsorption characteristics of anionic dye, new coccine (NC), onto α-Al_2O_3 beads with large size and predict adsorption mechanisms with adsorbed structure of NC molecules onto α-Al_2O_3. The influence of NC adsorption on the charging behavior of α-Al_2O_3 is determined by streaming potential. The surface modification of α-Al_2O_3 beads after NC adsorption is evaluated by Fourier transform infrared spectroscopy with attenuated total reflection technique (FTIR-ATR). To our best knowledge, this is the first systematic study in NC/Al_2O_3 system to relate electrokinetic and FTIR-ATR measurements with adsorption isotherms fitted by the two-step model.

Experimental

Materials

High purity (99.5 %), α-Al_2O_3 beads (Hiraceramics, Japan) with a diameter of about 300 μm and a density of 3.82 g/cm^3, were used in this study. X-ray diffraction (XRD) using an X-ray diffractometer (Bruker D8 Advance) confirmed that our material contains mainly α-phase. The specific surface area was determined by the Brunauer–Emmett–Teller (BET) method using a surface area analyzer (Micromeritics, Gemini VII 2390) and found to be around 0.0041 m^2/g. The alpha alumina was treated before measurements as follows: The original α-Al_2O_3 was washed various times with 0.1 M NaOH before washing by ultrapure water to reach neutral pH. After that, α-Al_2O_3 was dried at 110 °C and was reactivated at 550 °C for 2 h. Finally, the treated α-Al_2O_3 was cooled in a desiccator at room temperature and stored in a polyethylene container.

Anionic dye, new coccine (NC, with purity higher than 85 %), from Wako Pure Chemical Industries was used as adsorbate in dye adsorption. The chemical structure and cartoon representation of NC were indicated in Fig. 1. The effect of ionic strength was studied by the addition of NaCl (Wako). In order to adjust pH of solutions, HCl and NaOH (volumetric analysis grade, Wako) were used. Other chemicals were purchased from Wako. Ultrapure water was used in preparing solutions and in all measurements (Millipore, Elix Advantage 5).

Adsorption isotherms

Adsorption isotherms were conducted by batch experiments in 100-mL Erlenmeyer flasks at 22±2 °C, controlled by an air-conditioner. To carry out adsorption experiments, 0.5 g of the treated α-Al_2O_3 was mixed with 25 mL of NaCl aqueous solutions at different concentrations by a shaker for 1 h. For NC adsorption studies, the concentration from 10^{-6} to 10^{-3} M was desired and pH was adjusted to original value. The equilibrium time in dye adsorption was achieved after 3 h, while the change in pH of all solutions during adsorption was not significant. The adsorption density of NC (Γ_{NC}) onto α-Al_2O_3 was determined by the different concentrations of NC solutions before adsorption and after equilibrium process by colorimetric method.

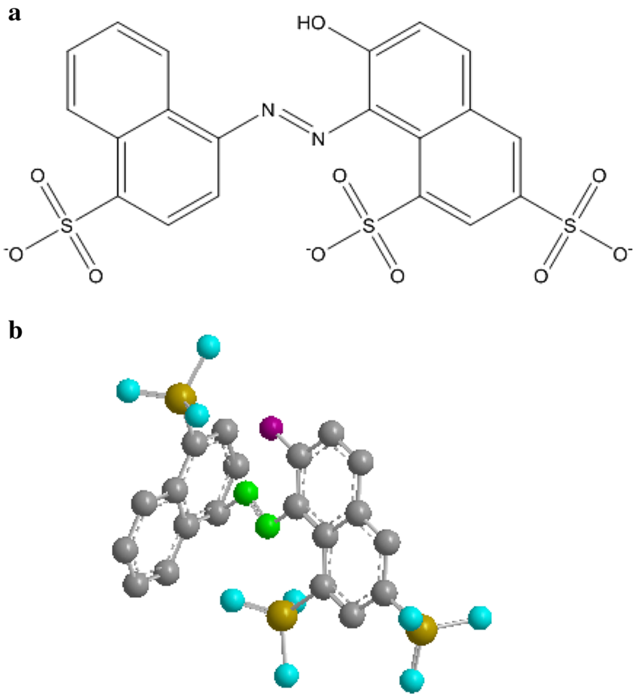

Fig. 1 The chemical structure (**a**) and cartoon representation (**b**) of anionic dye new coccine, NC

Colorimetric method

The concentration of anionic dye NC was analyzed by colorimetric method at a wavelength of 505 nm using an UV–vis spectrophotometer (UV-1650PC, Shimadzu) with a quartz cuvette with a 1-cm optical path length. The relationship between the absorbance and concentrations of NC as standard calibration curves in different electrolyte concentrations and pH with a correlation coefficient of at least 0.999 was confirmed. Samples were diluted appropriately before measuring the absorbance to quantify NC concentrations by standard calibration curves.

Potentiometric method

Potentiometric method was used to determine pH of all solutions. The method was carried out using a Metrohm 781 pH/Ion meter, Switzerland, by a glass combination electrode (Type 6.0258.010 Metrohm). We use three standard buffers (Metrohm) to calibrate the electrode before measuring pH of solutions. All measurements were carried out at 22±2 °C.

Streaming potential measurements

A streaming potential technique was applied to evaluate the change in surface charge by charactering the zeta potential of α-Al_2O_3 before and after adsorption of NC. The theory of streaming potential and ζ potential calculation were described in the literatures [39, 40]. In brief, the ζ potential from streaming potential is calculated by using Helmholtz–Smoluchowski's equation (HS) [39]:

$$\zeta = \frac{U_{str}}{\Delta P} \times \frac{\eta K_L}{\varepsilon \varepsilon_o} \quad (1)$$

where ζ is the zeta potential (mV), U_{str} is the different potential (mV), ΔP the pressure difference (mbar), η the viscosity of the solution (mPa.s), K_L the conductivity of the solution (mS/cm), ε the relative dielectric constant of the liquid and ε_o is the electric permittivity of vacuum (8.854×10^{-12} F/m).

Zeta CAD which is an instrument to evaluate zeta potential from the measurement of streaming potential is used in the present study. The detail of experimental procedure of streaming potential with Zeta CAD was described in our previously published paper [41]. Adsorption of NC onto α-Al_2O_3 was conducted with a solid-to-solution ratio of 200 g/L in 0.01 M NaCl at pH 4.0. The adsorption was conducted at the concentration of 10^{-3} M of NC. The α-Al_2O_3 beads after adsorption with NC were separated without washing and dried in air and then stored in a dark container until the measurement of streaming potential.

FTIR-ATR spectroscopy

To confirm surface modification of α-Al_2O_3 and to examine the structures of adsorbed NC, Fourier transform infrared spectroscopy was taken. The infrared spectra were performed by a Perkin Elmer GX FTIR spectrometer using a deuterated glycine sulfate (DTGS) detector. An attenuated total reflection (ATR) attachment with a micro germanium (Ge) crystal was used. The sample used to investigate the effect of NC adsorption was prepared as follows: The α-Al_2O_3 material (10 g) was equilibrated with the concentration of 10^{-3} M of NC in 50 mL solution of 0.01 M NaCl at pH 4 according to adsorption procedure in section 2.2. The α-Al_2O_3 sample after adsorption with NC was separated without rinsing and dried at about 70 °C and then kept in a dark container. The spectrum of NC powder was recorded without any treatment. All recorded spectra were obtained at 25 °C and atmospheric pressure at a resolution of 4 cm^{-1}.

General isotherm equation

Theory and modeling

The obtained isotherms were fitted by a general isotherm equation. The equation was derived by assuming that two steps of the adsorption can be obtained on solid–liquid interface [26, 42]. It was originally derived to describe the surfactant adsorption with hemimicelle formation.

The general isotherm equation is

$$\Gamma = \frac{\Gamma_\infty k_1 C\left(\frac{1}{n} + k_2 C^{n-1}\right)}{1 + k_1 C\left(1 + k_2 C^{n-1}\right)} \quad (2)$$

where Γ is amount of NC adsorbed, Γ_∞ is the maximum adsorption amount, k_1 and k_2 are equilibrium constants for the first-layer adsorption and clusters of n molecules or multilayer adsorption. C denotes the equilibrium concentration of NC in the dye solution.

Although the formation of micelle-like structure is not expected because of its structure [21], in the case of NC adsorption, this dye might adsorb in a cooperative manner to form cluster; the cooperative structure can be reflected in the parameter n.

Fitting procedure

The selected fitting parameters are described in the following: (a) Γ_∞ can be determined from the data of adsorption isotherm at high NC concentrations. (b) The k_1 can be predicted from the data of adsorption isotherm at low concentrations by a limiting Langmuir equation. (c) By using reasonable guesses for k_1 in step (b) and k_2 (with fixed one value of n), the calculation of the adsorption density Γ_{cal} for NC by Eq. (2) was calculated from experimental data points of C. (d) Procedure was repeated with 0.1 step change of n. (e) We use trial and error to find the minimum sum of square of residuals for every isotherm, $SS_{residuals}=\sum(\Gamma_{cal}-\Gamma_{exp})^2$, where Γ_{exp} is the experimental adsorption density of NC. (f) The minimum $SS_{residuals}$ was chosen to find the appropriate values for parameters k_1, k_2, and n.

Results and discussion

Streaming potential measurements

Zeta potential was determined by measuring streaming potential in the range from pH 4 to pH 9 to identify isoelectric point (IEP) of α-Al_2O_3 before and after adsorption of NC with Eq. (1). Figure 2 indicates the ζ potential of treated α-Al_2O_3 against pH in 0.01 M NaCl. The present IEP of α-Al_2O_3 without adsorption and NC (open triangles in Fig. 2) is around 6.7 [41].

The zeta potential of α-Al_2O_3 after NC adsorption (open circles in Fig. 2) decreases in the pH from 4 to 9 compared with the treated α-Al_2O_3 without NC adsorption. The values of ζ potential of α-Al_2O_3 decrease due to the presence of negative charges of sulfonic groups of azo dye. This trend of ζ potential is close to the values in literatures [24, 43, 44]. That is, Ramesh Kumar and Teli [43] indicated that in the presence of anionic azo dye, CI Direct Yellow 28, the streaming potential of cotton fibers has become more negative than that of raw one. Bourikas et al. [24] has revealed that the magnitude of ζ potential of TiO_2 in pH 2 to 8 in 0.01 M $NaNO_3$ reduced significantly in the presence of anionic dye, Acid Orange 7 (AO7), in solutions. The shift of IEP of AO7/TiO_2 suspensions was over 2 pH units. However, in our research, adsorption dye only induces a small shift of IEP (about 1 pH unit). It suggests that the interaction of NC with the surface of α-Al_2O_3 is not very strong. In other words, the inner-sphere complex between sulfonic groups and Al_2O_3 surface is not formed. The α-Al_2O_3 becomes less positively charged surface after NC adsorption although NC can be partly desorbed in the equilibrium process of streaming potential measurements. Therefore, the adsorption of NC still makes the decrease in surface charge of α-Al_2O_3.

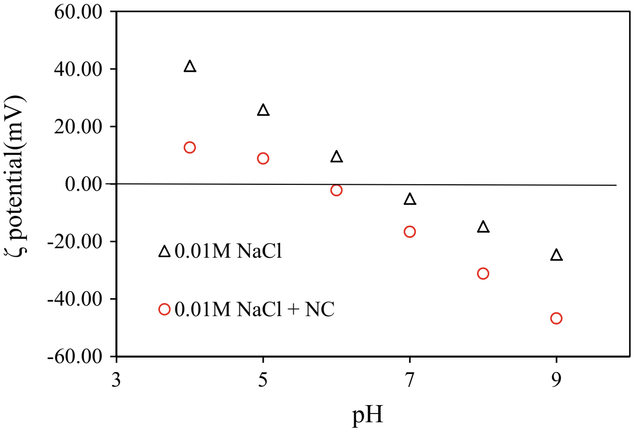

Fig. 2 The ζ potential of α-Al_2O_3 without adsorption (*open triangles*) and after NC adsorption (*open circles*) as a function of pH in 0.01 M NaCl

FTIR-ATR spectra

The Fourier transform infrared spectroscopy is often applied to characterize active groups in the adsorption. FTIR combined with attenuated total reflection for in situ of surface has become one of the powerful tools to explore the solid–liquid interface [45]. The ex situ FTIR-ATR spectra of α-Al_2O_3 beads without adsorption and after adsorption of NC (Al_2O_3-NC) have been assigned in the wavenumber range of 1000–2200 cm^{-1} shown in Fig. 3. The FTIR-ATR spectra of NC powder which has been also recorded from 1000 to 2200 cm^{-1} is given at the bottom of Fig. 3.

In Fig. 3, the large band at around 1612 cm^{-1} appeared in the spectra of Al_2O_3-NC. But the magnitude of this band is similar to another one of Al_2O_3 beads, demonstrating that increased amount of adsorbed water upon NC adsorption is not significant. The spectra of NC powder indicated that the bands at 1423, 1491, 1570, and 1632 cm^{-1} were assigned to the bond of C=C of naphthalene rings or phenyl ring vibration with stretching of the C=N group that corresponded to active

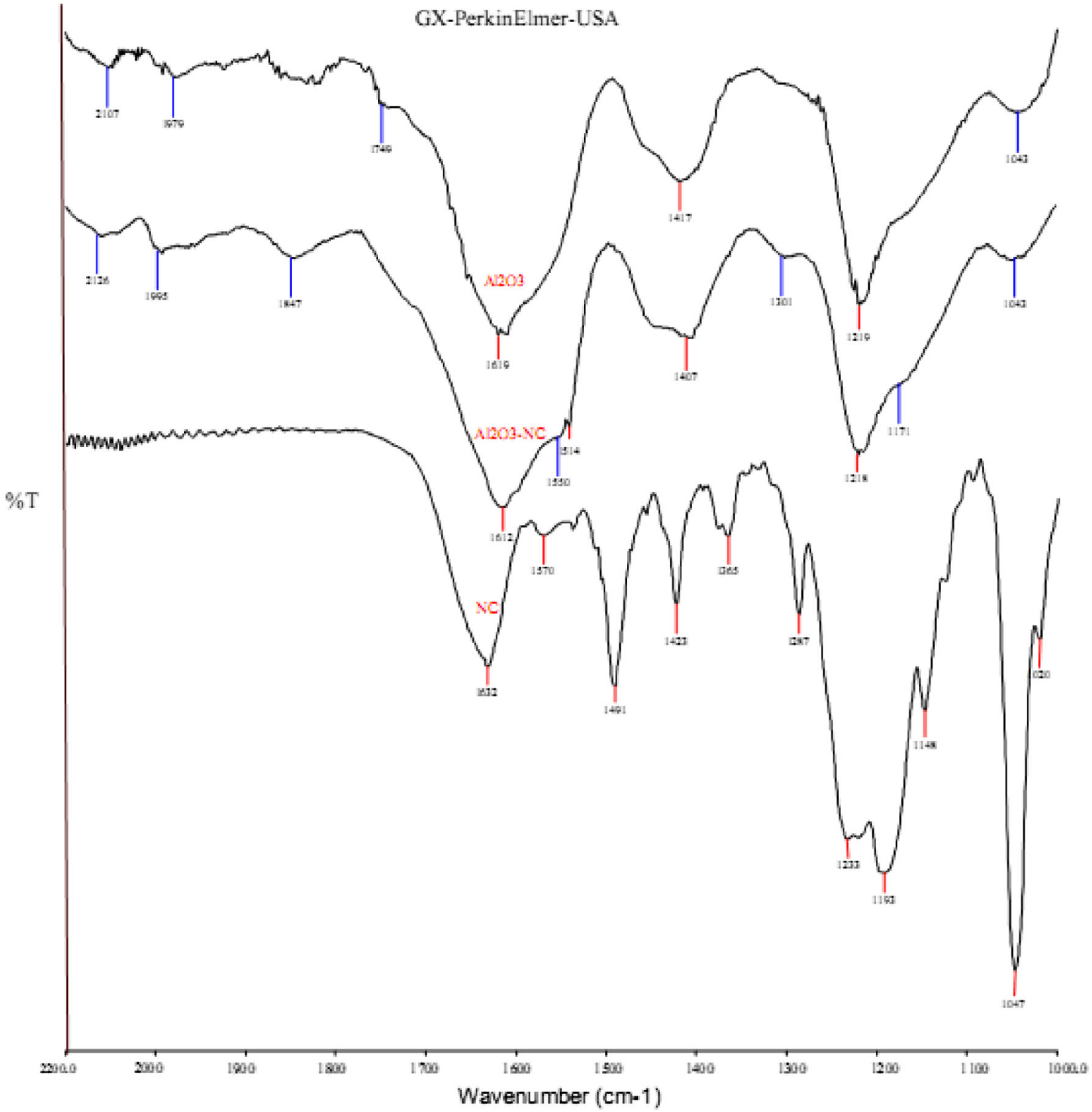

Fig. 3 FTIR-ATR spectra for α-Al_2O_3 without adsorption (Al_2O_3) and after NC adsorption (Al_2O_3-NC) and NC powder (NC) in the wavenumber range of 1000–2200 cm^{-1}

groups of azo dye. These bands are in good agreement with the spectra of NC [46]. The small appearance and the shifts of the bands were also seen in Fig. 3 with wavenumbers of 1407, 1514, and 1550 cm^{-1} appeared in the spectra of Al_2O_3-NC. Thus, the hydrophobic groups cannot contact the hydrophilic surface of alumina. It should be noted that the strong bands at 1193 and 1047 cm^{-1} corresponded to the vibrations of the O–S–(O_2) group [22, 24] of NC molecules disappeared in the spectra of Al_2O_3-NC. These results suggest the adsorption of NC molecules on Al_2O_3 by two oxygen atoms of sulfonic group of the azo dye [22, 24]. The FTIR-ATR spectra of α-Al_2O_3 and after adsorption of NC imply that the surface of α-Al_2O_3 is modified by adsorbed NC molecules via sulfonic groups. Therefore, we support that NC molecules mainly adsorb on the surface of α-Al_2O_3 by electrostatic attraction.

Adsorption of anionic azo dye onto large α-alumina beads

Adsorption isotherms of NC onto α-alumina discussed by two-step model

Adsorption isotherms of NC onto large α-Al_2O_3 beads with positively charged surface carried out at several pH values and different salt concentrations are indicated in Fig. 4. The influence of ionic strength is clearly observed at a given pH value. The NC adsorption density decreases with increasing ionic strength. This trend is close to the result of NC adsorption onto positively charged sludge particulates at pH <3 [21]. The increase in salt concentration increases the number of anions (counter ions) on the positively charged surface of α-Al_2O_3 beads, reducing the electrostatic effect of α-Al_2O_3

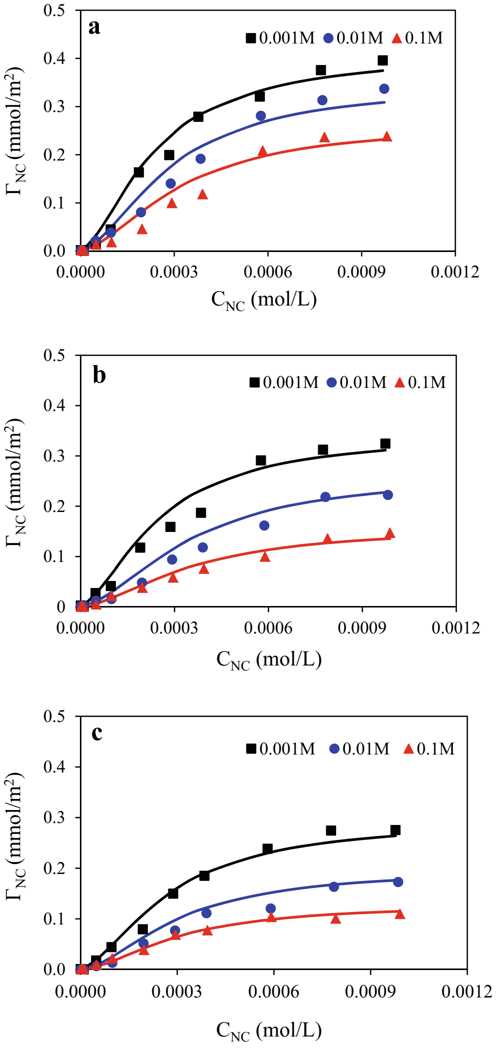

Fig. 4 Adsorption isotherms of NC onto α-Al_2O_3 at pH 4 (**a**), pH 5 (**b**), and pH 6 (**c**) and three salt concentrations. The *points* are experimental data while the *solid lines* are the results of two-step adsorption model

surface to dye molecules. In other words, the electrostatic attraction between the negative charge of sulfonic groups of NC dye and positive charge of α-Al_2O_3 surface is screened by increasing salt concentrations. The non-electrostatic interactions such as hydrophobic, proton binding, and Van der Waals are probably important in adsorption of organic anions onto the α-Al_2O_3 surface. However, adsorption of NC onto α-Al_2O_3 is mainly controlled by the electrostatic attraction so that adsorption decreases with increasing NaCl concentration. As seen from the isotherms in Fig. 4, at different pH and salt concentrations, the experimental results were fitted well by general isotherm equation Eq. (2) with the fit parameters in Table 1.

As shown in Table 1, increasing ionic strength induces a decrease in $k_{1,\mathrm{NC}}$ except for 0.1 M NaCl while a change in $k_{2,\mathrm{NC}}$ is not significant ($k_{2,\mathrm{NC}} \approx 8.0 \times 10^3$ m^2/mmol). The monolayer adsorption in the case of NC adsorption is influenced by ionic strength but the multilayer adsorption is not affected by ionic strength. It is hard to evaluate the number in multilayer adsorption for NC dye while the adsorbed structure at alumina/solution interface is based on the first layer. Thus, the number in multilayer adsorption was not determined in this study. Wang et al. [21] indicated that the adsorption of NC onto sludge particulates at different pH and ionic strength probably followed multilayer isotherm. In the paper [21], although the values of $k_{1,\mathrm{NC}}$ and $k_{2,\mathrm{NC}}$ are different from our results ($k_{1,\mathrm{NC}}$ is higher than $k_{2,\mathrm{NC}}$), the influence of ionic strength on isotherms seems to be similar to ours. Adsorption of NC onto sludge particles with high surface area reaches equilibrium in very fast time (about 30 min). On the other hand, NC adsorption onto large α-Al_2O_3 beads with small surface area takes long equilibrium time (after 180 min: not shown in detail). It implies that the specific surface area could promote equilibrium process of NC adsorption onto solid surface.

Figure 4 and Table 1 also show that adsorption density of dye strongly depends on pH and the equilibrium concentration of dye in solutions at a given ionic strength. Adsorption amount of NC onto α-Al_2O_3 beads increases with decreasing pH. The PZC of α-Al_2O_3 is about 6.7 and the decrease of pH induces an increase in the positive charge on surface of α-Al_2O_3. Since the NC dye has negative charge, the attractive force between anionic dye and positively charged surface α-Al_2O_3 is enhanced with a decrease in pH. These trends are similar to the adsorption of anionic dyes on positively charged metal oxides surface. Adsorption density of azo dyes with sulfonic group on metal oxide surfaces is reported [22, 24] in which adsorption density increases with decreasing pH and becomes not significant for pH>PZC. Furthermore, the change of pH upon NC adsorption is negligible or proton adsorption is not significant, meaning that the surface charge of α-Al_2O_3 is only affected by adsorbed amount of NC. Thus, the IEP of α-Al_2O_3 shifts to the lower pH after NC adsorption (see the streaming potential measurements).

The results of adsorption isotherms of anionic azo dye onto α-Al_2O_3 indicated above agree well with our electrokinetic and spectroscopic data are close to the results of previous researches [22, 24]. Nevertheless, the influence of ionic strength on adsorption of azo dyes on the metal oxides by experiment and modeling was not examined in published papers [22, 24]. On the one hand, the influences of pH and salt concentration to the adsorption of trivalent sulfonic dye, NC onto α-Al_2O_3 in our study are close to the results of Wang et al. [21] who investigated adsorption of NC onto sludge particulates. However, in the paper [21], the electrokinetic and spectroscopic data and structure of adsorbed NC have not been reported. In the present study, we succeeded in relating the electrokinetic and spectroscopic information with adsorption isotherms by two-step model to propose the structure of adsorbed NC onto α-Al_2O_3.

Table 1 The fit parameters for NC adsorption, which are maximum adsorbed amount $\Gamma_{\infty,\mathrm{NC}}$, the equilibrium constants $k_{1,\mathrm{NC}}$ and $k_{2,\mathrm{NC}}$ for first-layer adsorption and multilayer adsorption, respectively, and n_{NC} the number of cluster of NC molecules

C salt (M NaCl)	pH	$\Gamma_{\infty,\mathrm{NC}}$ (mmol/m^2)	$k_{1,\mathrm{NC}}$ (m^2/mmol)	$k_{2,\mathrm{NC}}$ (m^2/mmol)$^{n-1}$	n_{NC}
0.001	4	0.42	2.0×10^3	8.0×10^3	2
0.001	5	0.35	1.9×10^3	8.0×10^3	2
0.001	6	0.30	1.6×10^3	8.0×10^3	2
0.01	4	0.35	1.2×10^3	1.0×10^4	2
0.01	5	0.27	1.0×10^3	8.0×10^3	2
0.01	6	0.20	0.6×10^3	8.0×10^3	1.9
0.1	4	0.27	1.2×10^3	8.0×10^3	2
0.1	5	0.16	1.0×10^3	8.0×10^3	2
0.1	6	0.13	0.6×10^3	8.0×10^3	1.9

Structure of adsorbed NC onto α-Al_2O_3

The two-step model was established to describe the NC adsorption onto α-Al_2O_3, suggesting that dye adsorption could occur with cooperative manner. Adsorption of NC decreases with increasing pH due to a decrease of positive surface charge. During NC adsorption, the pH of all solutions does not change significantly, indicating that proton co-adsorption is negligible. Therefore, the net surface charge of NC-covered α-Al_2O_3 at fixed pH is dependent on the adsorption amount of NC. A small decrease of surface charge or small reduction of zeta potential was obtained by streaming potential, in accordant with low adsorption amount of NC, compared with adsorption of sodium dodecyl sulfate (SDS, anionic surfactant) [20]. We confirmed that adsorption of NC on the surface of α-Al_2O_3 occurs via only one sulfonic group of azo dye. It was supported by the results of FTIR-ATR spectra and adsorption isotherms. These results suggest that the adsorption of NC onto α-Al_2O_3 is mainly controlled by the electrostatic attraction between positive charges of α-Al_2O_3 surface and negative charges of sulfonic groups. In this case, a bridged bidentate complex can be formed [22] irrespective of salt concentrations. However, the formation of a bidentate inner sphere surface complex is not supported as the cases of adsorption of anionic dye, AO7 on the TiO_2 [24] or adsorption of azo dye, Orange G on α-Fe_2O_3 [22] because NC is easily desorbed in equilibrium and measuring processes of streaming potential. In streaming potential measurement, desorption of NC can be recognized from color change of α-Al_2O_3 beads packed in a glass column. Also, the NC desorption took place quickly at high salt concentration and high pH by batch experiment (not shown in detail). The proton co-adsorption upon the adsorption of organic ions is important to predict the mechanism and adsorbed structures. In our previously published papers, the concomitant proton adsorption is significant in the case of surfactant adsorption [20] while the proton co-adsorption upon polyelectrolye adsorption can also be determined [29]. Nevertheless, the adsorption amount of proton during adsorption of NC on α-Al_2O_3 is not significant after adjusting pH to original value. It is implied that the released proton amount does not induce to the mechanism of adsorption amount of NC.

The adsorption of NC was probably influenced by the positions of sulfonic group. In this research, we suggest that only one sulfonic group on the naphthalene ring without hydroxyl group of NC attaches to alumina in the adsorption while two sulfonic groups on another naphthalene ring do not contribute for adsorption. Figure 5 shows a cartoon representation of the adsorbed structure of NC onto α-Al_2O_3. In Fig. 5, a NC molecule adsorbed onto α-Al_2O_3 by one sulfonic group of anionic dye, creating a bridged bidentate complex between two aluminum ions and the surface oxygens. It is close to the description in reported paper of Bourikas et al. [24], who suggested the similar structure of the adsorbed AO7. The lower adsorption amount of NC onto α-Al_2O_3 can also be explained by the metal–metal distance and a crystalline face of metal oxide rather than specific surface area, although the surface area seems to be an important factor to control adsorption. In the paper [22], the same reason was found to demonstrate a higher adsorption of anionic azo dye Orange II on α-Fe_2O_3 than TiO_2 and Al_2O_3 oxides.

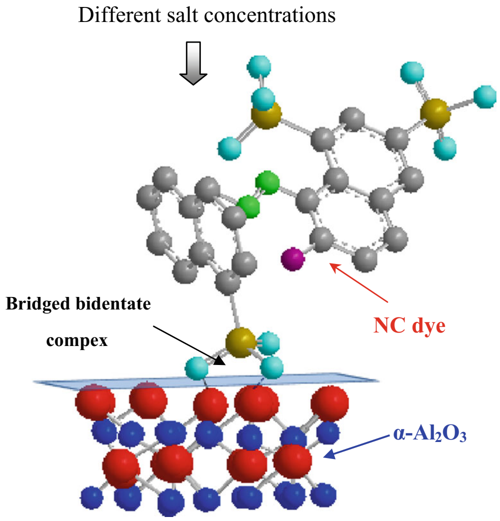

Fig. 5 Cartoon representation of structure of the adsorbed NC onto α-Al_2O_3. Two oxygen atoms of the sulfonic group on naphthalene ring favor the adsorption of NC dye by the bridged bidentate complex

Table 2 The fit parameters for SDS adsorption, which are maximum adsorbed amount $\Gamma_{\infty,\mathrm{SDS}}$, the equilibrium constants $k_{1,\mathrm{SDS}}$ and $k_{2,\mathrm{SDS}}$ for first step and second step, respectively, and n_{SDS} the aggregation number of hemimicelle [20]

C salt (M NaCl)	pH	$\Gamma_{\infty,\mathrm{SDS}}$ (mmol/m^2)	$k_{1,\mathrm{SDS}}$ (m^2/mmol)	$k_{2,\mathrm{SDS}}$ (m^2/mmol)$^{n-1}$	n_{SDS}
0.001	4	1.20	6×10^3	1×10^{24}	9.8
0.001	5	0.95	6×10^3	6×10^{23}	9.8
0.001	6	0.52	6×10^3	5×10^{23}	9.8
0.01	4	1.55	4×10^3	8×10^{23}	9.8
0.01	5	1.10	4×10^3	7×10^{23}	9.8
0.01	6	0.65	4×10^3	6×10^{23}	9.9
0.1	4	1.67	1×10^3	6×10^{22}	10.1
0.1	5	1.40	1×10^3	5×10^{22}	10.1
0.1	6	0.77	1×10^3	4×10^{22}	10.1

Comparison of differences between anionic dye adsorption and anionic surfactant adsorption

In this part, we compare the differences in adsorption characteristics between anionic azo dye, NC, and anionic surfactant SDS in order to better understand the adsorption in natural aqueous media.

Although adsorption experiments of both SDS and NC were carried out in similar conditions (initial pH and salt concentrations), the adsorption isotherms were different in some points as follows: At a given pH, the NC adsorption increases with decreasing NaCl concentration. Nevertheless, the adsorption isotherms SDS onto α-Al_2O_3 at three salt concentrations show a common intersection point (CIP). The CIP results from charge adjustment as well as the presence of hydrophobic interactions [20]. Above the CIP, the salt effect is reversed and the adsorption density of SDS decreases at lower ionic strength.

The experimental results of both SDS and NC adsorption isotherms onto α-Al_2O_3 were reasonably represented by two-step adsorption model. According to the results of our previous work [20], we show again the fit parameters and experimental data for SDS adsorption in Table 2. As can be seen, Tables 1 and 2 indicate that the maximum adsorption density of NC ($\Gamma_{\infty\mathrm{NC}}$) is much lower than the one of SDS ($\Gamma_{\infty\mathrm{SDS}}$) at the same conditions, although molecular weight of NC is about two times higher than molecular weight of SDS. For SDS adsorption, the micelles are formed with aggregation numbers of hemimicelle ($n_{\mathrm{SDS}}\approx10$) that are about five times higher than n_{NC} ($n_{\mathrm{NC}}\approx2$) for NC adsorption. It can also be observed that the values of $k_{1,\mathrm{NC}}$ and $k_{1,\mathrm{SDS}}$ are not very different, while the values of $k_{2,\mathrm{SDS}}$ are greatly higher than $k_{2,\mathrm{NC}}$ (10^{19} to 10^{20} times). These results reveal that micellization of NC cannot occur on the surface of α-Al_2O_3 as well as on sludge particulates [21].

Another feature is that the adsorption of anionic surfactants onto metal oxides can induce the proton co-adsorption [17, 20, 47], while the adsorption of anionic dye does not affect proton adsorption. Therefore, the SDS adsorption shifts the isoelectric point (IEP) to higher pH. On the one hand, the NC adsorption decreases the IEP to lower pH (streaming potential measurements section). Furthermore, the FTIR-ATR spectra of α-Al_2O_3 beads without adsorption and after adsorption of NC (see FTIR-ATR spectra section) compared with the spectra of α-Al_2O_3 after adsorption of SDS suggested that NC mainly adsorbed on the surface of α-Al_2O_3 by electrostatic attraction while the adsorption of SDS molecules were driven by both electrostatic and hydrophobic interactions.

Conclusions

We have analyzed adsorption properties of anionic azo dye, NC, onto α-alumina with large size. Streaming potential indicated that the IEP of α-Al_2O_3 shifts to the lower pH after adsorption of NC because of the adsorption of negatively charged sulfonic group of the dye. FTIR-ATR confirmed the presence and absence of different active groups of NC on the surface of α-Al_2O_3. The two-step model was successfully applied to represent the experimental results of adsorption isotherms of NC onto α-Al_2O_3. Adsorption density of NC increased with decreasing pH due to an increase in initial positive surface charge of α-Al_2O_3. At a given pH value, the adsorption amounts of NC decreased with increasing salt concentration, confirming that the NC adsorption onto α-Al_2O_3 is mainly induced by electrostatic attraction. The results of adsorption isotherms, the zeta potential change, and the surface modifications suggested that adsorption of NC is affected by the formation between only one sulfonic group on the naphthalene ring and the surface of α-Al_2O_3. We suggest that a bridged bidentate complex of two oxygen ions of sulfonic group and aluminum ions induced the adsorption of NC onto α-Al_2O_3.

Acknowledgments We would like to thank the financial support from JSPS KAKENHI (22248025, 23688027).

References

1. Adak A, Bandyopadhyay M, Pal A (2005) Removal of crystal violet dye from wastewater by surfactant-modified alumina. Sep Purif Technol 44(2):139–144
2. Wong YC, Szeto YS, Cheung WH, McKay G (2003) Equilibrium studies for acid dye adsorption onto chitosan. Langmuir 19(19): 7888–7894
3. Forgacs E, Cserháti T, Oros G (2004) Removal of synthetic dyes from wastewaters: a review. Environ Int 30(7):953–971
4. Gupta VK, Suhas (2009) Application of low-cost adsorbents for dye removal—a review. J Environ Manag 90(8):2313–2342
5. Almeida CAP, Debacher NA, Downs AJ, Cottet L, Mello CAD (2009) Removal of methylene blue from colored effluents by adsorption on montmorillonite clay. J Colloid Interface Sci 332(1): 46–53
6. Doğan M, Alkan M, Türkyilmaz A, Özdemir Y (2004) Kinetics and mechanism of removal of methylene blue by adsorption onto perlite. J Hazard Mater 109(1–3):141–148
7. Hameed BH, El-Khaiary MI (2008) Removal of basic dye from aqueous medium using a novel agricultural waste material: pumpkin seed hull. J Hazard Mater 155(3):601–609
8. Schoonen MA, Schoonen JMT (2014) Removal of crystal violet from aqueous solutions using coal. J Colloid Interface Sci 422:1–8
9. Al-Momani F, Touraud E, Degorce-Dumas JR, Roussy J, Thomas O (2002) Biodegradability enhancement of textile dyes and textile wastewater by VUV photolysis. J Photochem Photobiol A Chem 153(1–3):191–197
10. Kang S-F, Liao C-H, Po S-T (2000) Decolorization of textile wastewater by photo-fenton oxidation technology. Chemosphere 41(8): 1287–1294
11. Pérez M, Torrades F, Domènech X, Peral J (2002) Fenton and photo-fenton oxidation of textile effluents. Water Res 36(11): 2703–2710
12. Mohan N, Balasubramanian N, Basha CA (2007) Electrochemical oxidation of textile wastewater and its reuse. J Hazard Mater 147(1–2):644–651
13. Vlyssides AG, Loizidou M, Karlis PK, Zorpas AA, Papaioannou D (1999) Electrochemical oxidation of a textile dye wastewater using a Pt/Ti electrode. J Hazard Mater 70(1–2):41–52
14. Papić S, Koprivanac N, Lončarić Božić A, Meteš A (2004) Removal of some reactive dyes from synthetic wastewater by combined Al(III) coagulation/carbon adsorption process. Dyes Pigments 62(3):291–298
15. Ledakowicz S, Solecka M, Zylla R (2001) Biodegradation, decolourisation and detoxification of textile wastewater enhanced by advanced oxidation processes. J Biotechnol 89(2–3):175–184
16. Hameed BH, El-Khaiary MI (2008) Batch removal of malachite green from aqueous solutions by adsorption on oil palm trunk fibre: equilibrium isotherms and kinetic studies. J Hazard Mater 154(1–3):237–244
17. Bohmer MR, Koopal LK (1992) Adsorption of ionic surfactants on variable-charge surfaces. 1. Charge effects and structure of the adsorbed layer. Langmuir 8(11):2649–2659
18. Goloub TP, Koopal LK, Bijsterbosch BH, Sidorova MP (1996) Adsorption of cationic surfactants on silica. Surface charge effects. Langmuir 12(13):3188–3194
19. Koopal LK, Lee EM, Böhmer MR (1995) Adsorption of cationic and anionic surfactants on charged metal oxide surfaces. J Colloid Interface Sci 170(1):85–97
20. Pham TD, Kobayashi M, Adachi Y (2015) Adsorption of anionic surfactant sodium dodecyl sulfate onto alpha alumina with small surface area. Colloid Polym Sci 293(1):217–227
21. Wang J, Huang CP, Allen HE, Cha DK, Kim D-W (1998) Adsorption characteristics of dye onto sludge particulates. J Colloid Interface Sci 208(2):518–528
22. Bandara J, Mielczarski JA, Kiwi J (1999) 1. Molecular mechanism of surface recognition. Azo dyes degradation on Fe, Ti, and Al oxides through metal sulfonate complexes. Langmuir 15(22): 7670–7679
23. Bauer C, Jacques P, Kalt A (1999) Investigation of the interaction between a sulfonated azo dye (AO7) and a TiO_2 surface. Chem Phys Lett 307(5–6):397–406
24. Bourikas K, Stylidi M, Kondarides DI, Verykios XE (2005) Adsorption of acid orange 7 on the surface of titanium dioxide. Langmuir 21(20):9222–9230
25. Buergisser CS, Cernik M, Borkovec M, Sticher H (1993) Determination of nonlinear adsorption isotherms from column experiments: an alternative to batch studies. Environ Sci Technol 27(5):943–948
26. Zhu B-Y, Gu T (1991) Surfactant adsorption at solid-liquid interfaces. Adv Colloid Interf Sci 37(1–2):1–32
27. Hoffmann I, Oppel C, Gernert U, Barreleiro P, von Rybinski W, Gradzielski M (2012) Adsorption isotherms of cellulose-based polymers onto cotton fibers determined by means of a direct method of fluorescence spectroscopy. Langmuir 28(20):7695–7703
28. Ndong R, Russel W (2012) Linear viscoelasticity of ZrO_2 nanoparticle dispersions with associative polymers. Rheol Acta 51(9):771–782
29. Pham TD, Kobayashi M, Adachi Y (2014) Adsorption of Polyanion onto Large Alpha Alumina Beads with Variably Charged Surface. Advances in Physical Chemistry 2014:9
30. Barrett EP, Joyner LG, Halenda PP (1951) The determination of pore volume and area distributions in porous substances. I. Computations from nitrogen isotherms. J Am Chem Soc 73(1): 373–380
31. Doulati Ardejani F, Badii K, Limaee NY, Shafaei SZ, Mirhabibi AR (2008) Adsorption of direct red 80 dye from aqueous solution onto almond shells: effect of pH, initial concentration and shell type. J Hazard Mater 151(2–3):730–737
32. Kamari A, Ngah WSW, Chong MY, Cheah ML (2009) Sorption of acid dyes onto GLA and H2SO4 cross-linked chitosan beads. Desalination 249(3):1180–1189
33. Piccin JS, Gomes CS, Feris LA, Gutterres M (2012) Kinetics and isotherms of leather dye adsorption by tannery solid waste. Chem Eng J 183:30–38
34. Harris RG, Wells JD, Johnson BB (2001) Selective adsorption of dyes and other organic molecules to kaolinite and oxide surfaces. Colloids Surf A Physicochem Eng Asp 180(1–2):131–140
35. Jain VK, Mundhara GL, Tiwari JS (1988) Sorption—desorption studies of anionic dyes on alumina pretreated with acids. Colloids Surfaces 29(4):373–389
36. Yahyaei B, Azizian S (2012) Rapid adsorption of anionic dyes by ordered nanoporous alumina. Chem Eng J 209:589–596
37. Jada A, Akbour RA (2012) Transport of basic colorant through quartz sand. J Colloid Sci Biotechnol 1(1):26–32
38. Kobayashi M, Nanaumi H, Muto Y (2009) Initial deposition rate of latex particles in the packed bed of zirconia beads. Colloids Surf A Physicochem Eng Asp 347(1–3):2–7
39. Delgado AV, González-Caballero F, Hunter RJ, Koopal LK, Lyklema J (2007) Measurement and interpretation of electrokinetic phenomena. J Colloid Interface Sci 309(2):194–224
40. Hunter RJ (1981) Zeta potential in colloid science. Academic, London
41. Pham TD, Kobayashi M, Adachi Y (2013) Interfacial characterization of α-alumina with small surface area by streaming potential and chromatography. Colloids Surfaces A 436:148–157

42. Zhu B-Y, Gu T (1989) General isotherm equation for adsorption of surfactants at solid/liquid interfaces. Part 1. Theoretical. J Chem Soc, Faraday Trans 1: Phys Chem Condensed Phases 85(11): 3813–3817
43. Ramesh Kumar A, Teli MD (2007) Electrokinetic studies of modified cellulosic fibres. Colloids Surf A Physicochem Eng Asp 301(1–3):462–468
44. Ramos-Tejada MM, Ontiveros-Ortega A, Giménez-Martín E, Espinosa-Jiménez M, Molina Díaz A (2006) Effect of polyethyleneimine ion on the sorption of a reactive dye onto Leacril fabric: electrokinetic properties and surface free energy of the system. J Colloid Interface Sci 297(1):317–321
45. Hind AR, Bhargava SK, McKinnon A (2001) At the solid/liquid interface: FTIR/ATR—the tool of choice. Adv Colloid Interf Sci 93(1–3):91–114
46. Park IY, Kuroda K, Kato C (1990) Direct synthesis of intercalation compounds between a layered double hydroxide and an anionic dye. J Chem Soc Dalton Trans 10:3071–3074
47. Bitting D, Harwell JH (1987) Effects of counterions on surfactant surface aggregates at the alumina/aqueous solution interface. Langmuir 3(4):500–511